symmetry

MDPI

Article

Extremely Narrow Superconducting Band with Crystal Spin $\frac{3}{2}\hbar$ in LaH_{10}

Ekkehard Krüger

Institut für Materialwissenschaft, Materialphysik, Universität Stuttgart, D-70569 Stuttgart, Germany; ekkehard.krueger@imw.uni-stuttgart.de

Abstract: We show that the high-temperature superconductor LaH_{10} possesses an unusual superconducting band in its band structure. We examine this band by group-theoretical methods and report evidence that the special features of the band support the characteristics of the superconducting state in LaH_{10} at megabar pressures, i.e., the strong electron–phonon coupling and the high superconducting transition temperature.

Keywords: LaH_{10}; superconducting band; superconducting eigenstates; non-adiabatic Heisenberg model; group theory

1. Introduction

LaH_{10} is characterized by the high superconducting transition temperature of around 250 K at a pressure of about 170 GPa [1,2]. The superconducting properties of LaH_{10} are closely associated to the high symmetry of the cubic face-centered space group *Fm*3*m* (225) and the clathrate structure of the H atoms retaining the cubic face-centered symmetry [3,4]. The transition to superconductivity is not related to any structural transition [2]. All H vibrations can participate in the electron–phonon-coupling process, leading to a strong electron–phonon coupling, and the bonding between La and H atoms is characterized by ionic–covalent bonding [3,5,6]. The high superconducting transition temperature of LaH_{10} can be understood within the framework of classical theories, such as the Eliashberg theory [7].

These experimental and theoretical results provide an excellent basis for the application of the group-theoretical non-adiabatic Heisenberg model (NHM) to LaH_{10}. The NHM provides an additional aspect to the theory of superconductivity: the crystal spin of the localized electron and phonon states which operates in the non-adiabatic system. The conservation law of the crystal spin allows the Hamiltonian of the system to have superconducting *eigenstates* [8]. We show in this paper that the unusual superconducting properties of LaH_{10} are evidently related to the unusual superconducting band in the band structure of this material.

2. Superconducting Band in LaH_{10}

Figure 1 shows the conventional band structure of LaH_{10} as calculated by the FHI-aims program [9,10]. In principle, the NHM starts from such a "conventional" one-electron band structure calculation, which does not consider electronic correlation effects. The correlation effects responsible for the stable superconducting state are based on the three postulates of the group-theoretical NHM defining a strongly correlated non-adiabatic atomic-like motion at the Fermi level, see Section 4 of [8]. The NHM uses the symmetry of the Bloch states in the points of symmetry of the Brillouin zone. Since the FHI-aims program computes with spherical harmonics as basis functions, I am able to determine the symmetry of the Bloch functions by the symmetry of the spherical harmonics as given in [11].

check for updates

Citation: Krüger, E. Extremely Narrow Superconducting Band with Crystal Spin $\frac{3}{2}\hbar$ in LaH_{10}. *Symmetry* **2023**, *15*, 1533. https://doi.org/10.3390/sym15081533

Academic Editor: Vladimir A. Stephanovich

Received: 14 July 2023
Revised: 30 July 2023
Accepted: 1 August 2023
Published: 3 August 2023

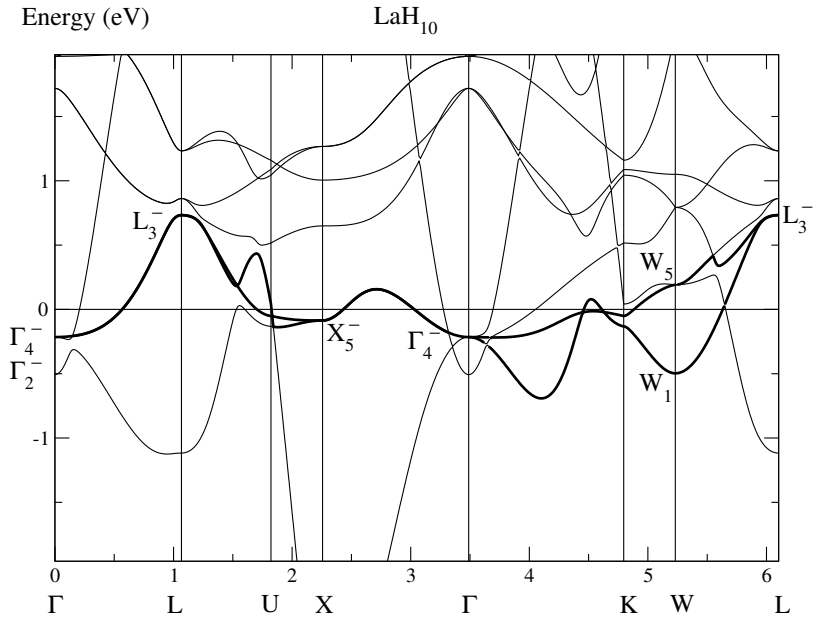

Figure 1. Conventional band structure of of LaH_{10} (i.e., the band structure does not take into account any electronic correlation effect) calculated by the FHI-aims program [9,10] using the length $a = 5.10$ Å (at 150 GPa) of the unit cell as given in [1]. The extremely narrow superconducting band is highlighted by the bold lines. Two H atoms in the unit cell are situated on the Wyckoff position c and have the coordinates $\big((1/4) * a, (1/4) * a, (1/4) * a\big)$ and $\big((1/4) * a, (1/4) * a, (3/4) * a\big)$, respectively. The remaining eight H atoms lie on the Wyckoff positions f involving the points (x, x, x) where x is not fixed by symmetry. We have chosen $x = \pm(1/8 - 1/32) * a$ for our band structure calculation because this choice yields the clearest result. The notations of the points of symmetry in the Brillouin zone for Γ_c^f follow Figure 3.14 of Ref. [11], and the symmetry notations are defined in Table A1 of Appendix A.

The band highlighted by the bold line is labeled by the single-valued representations

$$\Gamma_4^-, \quad L_3^-, \quad X_5^-, \quad \text{and} \quad W_5 + W_1. \tag{1}$$

It should be noted that, according to Definition 2 of [12], the highlighted band is a single closed band consisting of two branches.

From Table 1, we receive the corresponding double-valued representations

$$\begin{aligned} \Gamma_4^- \times \boldsymbol{d}_{1/2} &= \Gamma_6^- + \Gamma_8^- \\ L_3^- \times \boldsymbol{d}_{1/2} &= L_5^- + L_6^- + L_4^- \\ X_5^- \times \boldsymbol{d}_{1/2} &= X_6^- + X_7^- \\ W_5 \times \boldsymbol{d}_{1/2} &= W_6 + W_7 \\ W_1 \times \boldsymbol{d}_{1/2} &= W_6, \end{aligned} \tag{2}$$

where $\boldsymbol{d}_{1/2}$ denotes the two-dimensional double-valued representation of the three-dimensional rotation group $O(3)$ given, e.g., in Table 6.1 of [11]. The notations of the single-valued and double-valued representations are given in Tables A1 and A2, respectively, of Appendix A.

Table 1. Compatibility relations between the single-valued (upper row) and double-valued (lower row) representations of the space group $Fm3m$. Each column lists the double-valued representation $R_i \times \boldsymbol{d}_{1/2}$ below the single-valued representation R_i, where $\boldsymbol{d}_{1/2}$ denotes the two-dimensional double-valued representation of the three-dimensional rotation group $O(3)$ given, e.g., in Table 6.1 of [11].

$\Gamma(000)$										
Γ_1^+ Γ_6^+	Γ_2^+ Γ_7^+	Γ_2^- Γ_7^-	Γ_1^- Γ_6^-	Γ_3^+ Γ_8^+	Γ_3^- Γ_8^-	Γ_4^+ $\Gamma_6^+ + \Gamma_8^+$	Γ_5^+ $\Gamma_7^+ + \Gamma_8^+$	Γ_4^- $\Gamma_6^- + \Gamma_8^-$	Γ_5^- $\Gamma_7^- + \Gamma_8^-$	
$X(\frac{1}{2}0\frac{1}{2})$										
X_1^+ X_6^+	X_2^+ X_6^+	X_3^+ X_7^+	X_4^+ X_7^+	X_5^+ $X_6^+ + X_7^+$	X_1^- X_6^-	X_2^- X_6^-	X_3^- X_7^-	X_4^- X_7^-	X_5^- $X_6^- + X_7^-$	
$L(\frac{1}{2}\frac{1}{2}\frac{1}{2})$						$W(\frac{1}{2}\frac{1}{4}\frac{3}{4})$				
L_1^+ L_4^+	L_2^+ L_4^+	L_1^- L_4^-	L_2^- L_4^-	L_3^+ $L_5^+ + L_6^+ + L_4^+$	L_3^- $L_5^- + L_6^- + L_4^-$	W_1 W_6	W_2 W_6	W_3 W_7	W_4 W_7	W_5 $W_6 + W_7$

This list (2) contains each double-valued representation of Band 6 in Table 2. Thus, we may unitarily transform the Bloch functions of the band highlighted by the bold line into optimally localized spin-dependent Wannier functions centered at the La atoms. However, first, the rare *four*-dimensional Γ_8^- symmetry of these Wannier functions (and, consequently, of the non-adiabatic localized states) presents problems because it was not yet considered in former papers. This shall be made up in the following section.

Table 2. Double-valued representations at the four points of symmetry Γ, X, L, and W in Brillouin zone for the space group $Fm3m$. These representations define the six superconducting bands of LaH_{10}. The Bloch functions of a superconducting band can be unitarily transformed into optimally localized spin-dependent Wannier functions adapted to $Fm3m$ [12]. These Wannier functions are centered at the La atoms and have the symmetry given in the second column.

BandNr	**La(000)**	**Γ**	***X***	***L***	***W***
1	Γ_6^+	Γ_6^+	X_6^+	L_4^+	W_6
2	Γ_7^+	Γ_7^+	X_7^+	L_4^+	W_7
3	Γ_7^-	Γ_7^-	X_7^-	L_4^-	W_6
4	Γ_6^-	Γ_6^-	X_6^-	L_4^-	W_7
5	Γ_8^+	Γ_8^+	$X_6^+ + X_7^+$	$L_5^+ + L_6^+ + L_4^+$	$W_6 + W_7$
6	Γ_8^-	Γ_8^-	$X_6^- + X_7^-$	$L_5^- + L_6^- + L_4^-$	$W_6 + W_7$

3. Non-Adiabatic Heisenberg Model

The conservation law of crystal spin, which holds in narrow, approximately half-filled superconducting bands, is a very important characteristic of superconducting bands in the non-adiabatic system. The conservation of the crystal spin forces the electrons to form Cooper pairs (below a well-defined transition temperature T_c) because the total crystal spin is not conserved in any unpaired state. In this section, we show that the conservation of crystal spin is also valid in superconducting bands with non-adiabatic localized states $|\vec{R}m\rangle$ of the *four*-dimensional $\Gamma_8^\pm$ symmetry. However, in the four-dimensional case, it leads to a strong coupling of the electron spins to the phonons.

In superconducting bands, the related localized states are represented by spin-dependent Wannier functions. The spin dependence of these functions causes a coupling between the electrons and the phonons represented by a modified operator of Coulomb interaction

$$\begin{aligned} H_{Cb} \quad = \quad & \sum_{\vec{Q}\vec{R},lm} \langle \vec{Q}_1, l_1; \vec{Q}_2, l_2; \vec{R}_1, m_1; \vec{R}_2, m_2 | H_{Cb} | \vec{R}_1, m_1'; \vec{R}_2, m_2' \rangle \\ & \times b^\dagger_{\vec{Q}_1 l_1} b^\dagger_{\vec{Q}_2 l_2} c^\dagger_{\vec{R}_1 m_1} c^\dagger_{\vec{R}_2 m_2} c_{\vec{R}_2 m_2'} c_{\vec{R}_1 m_1'} + \text{H.c.} \end{aligned} \tag{3}$$

operating in the non-adiabatic system. The boson operators $b^{\dagger}_{\vec{Q}l}$ and the fermion operators $c^{\dagger}_{\vec{R}m}$ create localized non-adiabatic phonon and electron states $|\vec{Q}l\rangle$ and $|\vec{R}m\rangle$ at positions $\vec{Q}$ and $\vec{R}$, respectively, and the matrix elements

$$\langle \vec{Q}_1, l_1; \vec{Q}_2, l_2; \vec{R}_1, m_1; \vec{R}_2, m_2 | H_{Cb} | \vec{R}_1, m_1'; \vec{R}_2, m_2' \rangle \tag{4}$$

are integrals over non-adiabatic localized electron and phonon functions.

The highly complex non-adiabatic states $|\vec{R}m\rangle$ are unknown except for one important property: they have the same symmetry as the spin-dependent Wannier functions. Thus, the non-adiabatic system becomes amenable to group theory.

In an early paper [13], I defined the conservation law of crystal spin

$$l_1 + l_2 + m_1 + m_2 = m_1' + m_2' + 4n \tag{5}$$

that the non-vanishing matrix elements (4) of H_{Cb} satisfy (n is an integer). The numbers $l = +1, 0, -1$ and $m = +\frac{1}{2}, -\frac{1}{2}$ stand for the crystal spins of the non-adiabatic phonons and electrons, respectively.

Up to now [8], I believed that, in cubic materials, the value of the electronic crystal spin is $\frac{1}{2}\hbar$, i.e., the localized functions characterizing the superconducting band have (in cubic materials) the two dimensional $\Gamma_6^{\pm}$ or $\Gamma_7^{\pm}$ symmetry. However, in LaH_{10} I found for the first time a superconducting band evidently characterized by non-adiabatic localized states with the four-dimensional Γ_8^{-} symmetry. We now consider this case.

First, the approach (3) must be changed. Now the half-filled superconducting band is occupied by two electrons. Thus, the fermion operators $c^{\dagger}_{\vec{R}m}$ create localized states $|\vec{R}m\rangle$ comprising an electron pair. So, two pairs of phonons result from the motion of the center of mass of one localized state $|\vec{R}m\rangle$, resulting in the new ansatz

$$\begin{aligned} H_{Cb} \quad = \quad & \sum_{\vec{Q}\vec{R},lm} \langle \vec{Q}_1', l_1'; \vec{Q}_2', l_2'; \vec{Q}_1, l_1; \vec{Q}_2, l_2; \vec{R}_1, m_1; \vec{R}_2, m_2 | H_{Cb} | \vec{R}_1, m_1'; \vec{R}_2, m_2' \rangle \\ & \times b^{\dagger}_{\vec{Q}_1' l_1'} b^{\dagger}_{\vec{Q}_2' l_2'} b^{\dagger}_{\vec{Q}_1 l_1} b^{\dagger}_{\vec{Q}_2 l_2} c^{\dagger}_{\vec{R}_1 m_1} c^{\dagger}_{\vec{R}_2 m_2} c_{\vec{R}_2 m_2'} c_{\vec{R}_1 m_1'} + \text{H.c.} \end{aligned} \tag{6}$$

where now $c^{\dagger}_{\vec{R}m}$ creates an electron pair in the non-adiabatic state $|\vec{R}m\rangle$ with $\Gamma_8^{\pm}$ symmetry.

The conservation of the crystal spin is expressed by the commutator

$$[H_{Cb}, M(\alpha)] = 0 \text{ for } \alpha \in G_0, \tag{7}$$

where G_0 denotes the point group of the system. The point group operator $M(\alpha)$ acts on both the non-adiabatic localized phonons according to

$$M(\alpha) b^{\dagger}_{\vec{Q}l} M(\alpha)^{\dagger} = \sum_{\mu} D_{\mu l}(\alpha) b^{\dagger}_{\vec{Q}\mu} \tag{8}$$

and the non-adiabatic localized electrons according to

$$M(\alpha) c^{\dagger}_{\vec{R}m} M(\alpha)^{\dagger} = \sum_{\nu} D_{\nu m}(\alpha) c^{\dagger}_{\vec{R}\nu}, \tag{9}$$

see Ref. [13]. The numbers $D_{\mu l}(\alpha)$ and $D_{\nu m}(\alpha)$ belong to a representation of G_0 of the localized phonons $b^{\dagger}_{\vec{Q}l}$ and the localized electrons $c^{\dagger}_{\vec{R}m}$, respectively. The phonons belong (in any case) to Γ_{15} [14], the localized electrons now belong to a four-dimensional (double valued) representation $\Gamma_8^{\pm}$. It should be noted that the conservation of the crystal spin, expressed by Equation (7), is not a consequence of the of the symmetry of the system. Thus, (7) is a (self-evident [13]) postulate of the NHM which has been shown to be true in the past, because we have not yet found any superconductor which is not connected with a superconducting band [8].

Consider the group

$$C_4 = \{E\ C_{4z}^{+}\ C_{2z}\ C_{4z}^{-}\} \tag{10}$$

of the rotations about the z axis and assume the representations Γ_{15} and $\Gamma_8^{\pm}$ of the non-adiabatic states to be diagonal for the point group operations $\alpha \in C_4$. Then, the crystal spin lays in z direction and we have

$$M(\alpha) b^{\dagger}_{\vec{Q}_1' l_1'} b^{\dagger}_{\vec{Q}_2' l_2'} b^{\dagger}_{\vec{Q}_1 l_1} b^{\dagger}_{\vec{Q}_2 l_2} c^{\dagger}_{\vec{R}_1 m_1} c^{\dagger}_{\vec{R}_2 m_2} c_{\vec{R}_2 m_2'} c_{\vec{R}_1 m_1'} M(\alpha)^{\dagger} = \lambda b^{\dagger}_{\vec{Q}_1' l_1'} b^{\dagger}_{\vec{Q}_2' l_2'} b^{\dagger}_{\vec{Q}_1 l_1} b^{\dagger}_{\vec{Q}_2 l_2} c^{\dagger}_{\vec{R}_1 m_1} c^{\dagger}_{\vec{R}_2 m_2} c_{\vec{R}_2 m_2'} c_{\vec{R}_1 m_1'} \tag{11}$$

for $\alpha \in C_4$, where

$$\lambda = D_{l_1' l_1'}(\alpha) D_{l_2' l_2'}(\alpha) D_{l_1 l_1}(\alpha) D_{l_2 l_2}(\alpha) D_{m_1 m_1}(\alpha) D_{m_2 m_2}(\alpha) D^{*}_{m_2' m_2'}(\alpha) D^{*}_{m_1' m_1'}(\alpha). \tag{12}$$

The conservation of the crystal spin in Equation (7) is satisfied if $\lambda = 1$. The numbers $D_{ll}(\alpha)$ and $D_{mm}(\alpha)$ are given in Table 3. Using these numbers, it can be deduced that $\lambda = 1$ if and only if

$$l_1' + l_2' + l_1 + l_2 + m_1 + m_2 = m_1' + m_2' + 4n \tag{13}$$

where $l = +1, 0, -1$ and $m = +3/2, +1/2, -1/2, -3/2$, as given in the left column of Table 3, and n is still an integer. Table 3 is an extension of Table I in [13].

Table 3. Representations of the crystallographic point group C_4 (Table 6.5 of [11]) subduced by $\Gamma_8^{\pm}$ and Γ_{15}. If m and l are indicated according to the left column, Equation (13) follows from the numbers $D_{mm}(\alpha)$ and $D_{ll}(\alpha)$ for $\alpha = C_{4z}^{\pm}$ and $\alpha = \overline{C}_{4z}^{\pm}$. From C_z and $\overline{C}_z$ alone follows a modified equation valid in (orthorhombic) crystals not containing a fourfold rotation axis. $\omega = (1+i)/\sqrt{2}$.

$D_{mm}(\alpha)$			E	$\overline{E}$	C_{4z}^{+}	$\overline{C}_{4z}^{+}$	C_{2z}	$\overline{C}_{2z}$	C_{4z}^{-}	$\overline{C}_{4z}^{-}$
m	=	$3/2$	1	-1	ω^*	$-\omega^*$	i	$-i$	ω	$-\omega$
m	=	$1/2$	1	-1	$-\omega$	ω	$-i$	i	$-\omega^*$	ω^*
m	=	$-1/2$	1	-1	$-\omega^*$	ω^*	i	$-i$	$-\omega$	ω
m	=	$-3/2$	1	-1	ω	$-\omega$	$-i$	i	ω^*	$-\omega^*$
$D_{ll}(\alpha)$										
l	=	1	1	1	i	i	-1	-1	$-i$	$-i$
l	=	0	1	1	1	1	1	1	1	1
l	=	-1	1	1	$-i$	$-i$	-1	-1	i	i

Thus, also the new Coulomb interaction in Equation (6) satisfies the conservation law (13) of crystal spin. Consequently, in the superconducting band characterized by localized states of $\Gamma_8^{\pm}$ symmetry, the electrons are forced to form Cooper pairs just as in superconducting bands characterized by the two-dimensional $\Gamma_6^{\pm}$ and $\Gamma_7^{\pm}$ symmetry. Table 3 confirms directly that the two electrons occupying a localized $\Gamma_8^{\pm}$ state, in the non-adiabatic system, behave like a single fermion with the crystal spin $\frac{3}{2}\hbar$.

4. Results

The paper shows that LaH_{10} possesses in its conventional band structure a superconducting band with two striking features:

(i) It is extremely narrow. Its band width is not greater than $\pm\frac{1}{2}$eV.

(ii) It is characterized by non-adiabatic localized states of the *four*-dimensional Γ_8^{-} symmetry. Just as electrons with the two-dimensional $\Gamma_6^{\pm}$ or $\Gamma_7^{\pm}$ symmetry (solely considered so far), electron pairs with the four-dimensional $\Gamma_8^{\pm}$ symmetry also conserve the crystal spin expressed by Equation (13) during the interaction with phonons. In this context, a pair of electrons, which occupies a $\Gamma_8^{\pm}$ state, behaves in the non-adiabatic system like a fermion with the crystal spin $\frac{3}{2}\hbar$. It may take the four directions $m = +3/2, +1/2, -1/2, -3/2$. Besides, one electron pair occupying a $\Gamma_8^{\pm}$ state generates or annihilates two phonon pairs during the interaction.

5. Discussion

Both features (i) and (ii) of the superconducting band presented in the foregoing Section 4 effect an increase of the superconducting transition temperature T_c:

(i) The width of the superconducting band has a great influence on the superconducting transition temperature T_c. The narrower the superconducting band, the higher the T_c is [8]. The physical background is that the mean time-of-stay for an electron in the non-adiabatic localized state increases with decreasing bandwidth, thereby increasing the atomic-like character.

(ii) The superconducting transition temperature increases with increasing density of states of the interacting electrons at the Fermi level. In the superconducting band with crystal spin $\frac{3}{2}\hbar$, twice the number of electrons are coupled to two phonon pairs. Thus, the electron phonon coupling is twice as big as in a superconducting band with crystal spin $\frac{1}{2}\hbar$, as is experimentally well confirmed in LaH_{10} [3,5,15]. A four-dimensional non-adiabatic $\Gamma_8^{\pm}$ state exists in the 24 cubic crystals listed in Table 4. The strong electron phonon coupling disappears when the symmetry of the crystal is disturbed. This theoretical result confirms the experimental observation of Feng Peng et al. that the superconducting properties of LaH_{10} are closely associated to the high symmetry of the cubic face-centered space group $Fm3m$ [3]. Sun et al. found experimentally that, at the transition from the space group $Fm3m$ to the monoclinic space group $C2/m$ (at the abrupt decompression from 138 to 120 GPa), the superconducting transition temperature in LaH_{10} decreases by about 20% (from 241 to 189 K) [4]. I ascribe this absolutely reversible process to a splitting of the four-dimensional localized Γ_8^- state in the monoclinic phase, which should be accompanied by a decrease of the electron-phonon coupling.

Table 4. The 24 cubic space groups containing at least one four-dimensional double-valued representation at point Γ. Thus, these space groups allow a superconducting band of strong electron-phonon coupling of the type LaH_{10}.

$P432$	$P4_232$	$F432$	$F4_132$	$I432$	$P4_332$	$P4_132$	$I4_132$
$P\bar{4}3m$	$F\bar{4}3m$	$I\bar{4}3m$	$P\bar{4}3n$	$F\bar{4}3c$	$I\bar{4}3d$	$Pm3m$	$Pn3n$
$Pm3n$	$Pn3m$	$Fm3m$	$Fm3c$	$Fd3m$	$Fd3c$	$Im3m$	$Ia3d$

The present work is limited to non-hexagonal materials that can produce a superconducting state of the LaH_{10} type. Although the *hcp* structure (with the space group $P6_3/mmc$) does not have four-dimensional double-valued representations at the point Γ, it also possesses superconducting bands that may produce a strong electron-phonon coupling. This is in accordance with recent experimental findings that high-T_c superconductivity may exist in hydrogen clathrate structures of *hcp* symmetry, too [16–18]. Superconducting bands in the *hcp* clathrate structure under pressure shall be discussed in a later paper.

Funding: This publication was supported by the Open Access Publishing Fund of the University of Stuttgart.

Data Availability Statement: All data used in the paper are listed in the tables. Additional data, such as superconducting or magnetic bands in other materials, are available from the author.

Acknowledgments: I am much indebted to Guido Schmitz for his continuing support of my work.

Conflicts of Interest: The author declares no conflict of interest.

Appendix A. Character Tables

This Appendix A provides the Tables of the single-valued and double-valued characters of the space group $Fm3m$ (225) of LaH_{10}. They define the notations of the representations used in the paper.

Table A1. Character tables of the single-valued irreducible representations of the space group $Fm3m = \Gamma_c^f O_h^5$ (225) determined from Table 5.7 of [11].

					$\Gamma(000)$					
	E	I	σ_m	C_{2m}	$C_{3j}^{\pm}$	$S_{6j}^{\pm}$	$C_{4m}^{\pm}$	$S_{4m}^{\pm}$	C_{2p}	σ_{dp}
Γ_1^+	1	1	1	1	1	1	1	1	1	1
Γ_2^+	1	1	1	1	1	1	−1	−1	−1	−1
Γ_2^-	1	−1	−1	1	1	−1	−1	1	−1	1
Γ_1^-	1	−1	−1	1	1	−1	1	−1	1	−1
Γ_3^+	2	2	2	2	−1	−1	0	0	0	0
Γ_3^-	2	−2	−2	2	−1	1	0	0	0	0
Γ_4^+	3	3	−1	−1	0	0	1	1	−1	−1
Γ_5^+	3	3	−1	−1	0	0	−1	−1	1	1
Γ_4^-	3	−3	1	−1	0	0	1	−1	−1	1
Γ_5^-	3	−3	1	−1	0	0	−1	1	1	−1

$m = x, y, z; \quad p = a, b, c, d, e, f; \quad j = 1, 2, 3, 4.$

			$L(\frac{1}{2}\frac{1}{2}\frac{1}{2})$			
	E	I	S_{61}^{-} S_{61}^{+}	C_{31}^{-} C_{31}^{+}	C_{2e} C_{2f} C_{2b}	σ_{db} σ_{de} σ_{df}
L_1^+	1	1	1	1	1	1
L_2^+	1	1	1	1	−1	−1
L_1^-	1	−1	−1	1	1	−1
L_2^-	1	−1	−1	1	−1	1
L_3^+	2	2	−1	−1	0	0
L_3^-	2	−2	1	−1	0	0

					$X(\frac{1}{2}0\frac{1}{2})$					
	E	C_{2y}	C_{4y}^{-} C_{4y}^{+}	C_{2z} C_{2x}	C_{2c} C_{2e}	I	σ_y	S_{4y}^{+} S_{4y}^{-}	σ_z σ_x	σ_{dc} σ_{de}
X_1^+	1	1	1	1	1	1	1	1	1	1
X_2^+	1	1	1	−1	−1	1	1	1	−1	−1
X_3^+	1	1	−1	1	−1	1	1	−1	1	−1
X_4^+	1	1	−1	−1	1	1	1	−1	−1	1
X_5^+	2	−2	0	0	0	2	−2	0	0	0
X_1^-	1	1	1	1	1	−1	−1	−1	−1	−1
X_2^-	1	1	1	−1	−1	−1	−1	−1	1	1
X_3^-	1	1	−1	1	−1	−1	−1	1	−1	1
X_4^-	1	1	−1	−1	1	−1	−1	1	1	−1
X_5^-	2	−2	0	0	0	−2	2	0	0	0

			$W(\frac{1}{2}\frac{1}{4}\frac{3}{4})$		
	E	C_{2x}	S_{4x}^{-} S_{4x}^{+}	C_{2f} C_{2d}	σ_z σ_y
W_1	1	1	1	1	1
W_2	1	1	1	−1	−1
W_3	1	1	−1	1	−1
W_4	1	1	−1	−1	1
W_5	2	−2	0	0	0

Table A2. Character tables of the double-valued irreducible representations of the space group $Fm3m = \Gamma_c^f O_h^5$ (225) determined from Table 6.13 of [11].

								$\Gamma(000)$								
			C_{2m}					C_{2p}			σ_m					σ_{dp}
	E	$\overline{E}$	$\overline{C}_{2m}$	$C_{3j}^{\pm}$	$\overline{C}_{3j}^{\pm}$	$C_{4m}^{\pm}$	$\overline{C}_{4m}^{\pm}$	$\overline{C}_{2p}$	I	$\overline{I}$	$\overline{\sigma}_m$	$S_{6j}^{\pm}$	$\overline{S}_{6j}^{\pm}$	$S_{4m}^{\pm}$	$\overline{S}_{4m}^{\pm}$	$\overline{\sigma}_{dp}$
Γ_6^+	2	−2	0	1	−1	$\sqrt{2}$	$-\sqrt{2}$	0	2	−2	0	1	−1	$\sqrt{2}$	$-\sqrt{2}$	0
Γ_7^+	2	−2	0	1	−1	$-\sqrt{2}$	$\sqrt{2}$	0	2	−2	0	1	−1	$-\sqrt{2}$	$\sqrt{2}$	0
Γ_8^+	4	−4	0	−1	1	0	0	0	4	−4	0	−1	1	0	0	0
Γ_6^-	2	−2	0	1	−1	$\sqrt{2}$	$-\sqrt{2}$	0	−2	2	0	−1	1	$-\sqrt{2}$	$\sqrt{2}$	0
Γ_7^-	2	−2	0	1	−1	$-\sqrt{2}$	$\sqrt{2}$	0	−2	2	0	−1	1	$\sqrt{2}$	$-\sqrt{2}$	0
Γ_8^-	4	−4	0	−1	1	0	0	0	−4	4	0	1	−1	0	0	0

$m = x, y, z; \quad p = a, b, c, d, e, f; \quad j = 1, 2, 3, 4.$

							$X(\frac{1}{2}0\frac{1}{2})$									
						$\overline{C}_{2x}$	$\overline{C}_{2c}$							$\overline{\sigma}_x$	σ_{dc}	
			C_{2y}	C_{4y}^-	$\overline{C}_{4y}^+$	C_{2z}	$\overline{C}_{2e}$			σ_y	S_{4y}^+	$\overline{S}_{4y}^-$	σ_z	$\overline{\sigma}_{de}$		
	E	$\overline{E}$	$\overline{C}_{2y}$	C_{4y}^+	$\overline{C}_{4y}^-$	$\overline{C}_{2z}$	$\overline{C}_{2c}$	I	$\overline{I}$	$\overline{\sigma}_y$	S_{4y}^-	$\overline{S}_{4y}^+$	$\overline{\sigma}_z$	σ_x	$\overline{\sigma}_{dc}$	σ_{de}
X_6^+	2	−2	0	$\sqrt{2}$	$-\sqrt{2}$	0	0	2	−2	0	$\sqrt{2}$	$-\sqrt{2}$	0	0		
X_7^+	2	−2	0	$-\sqrt{2}$	$\sqrt{2}$	0	0	2	−2	0	$-\sqrt{2}$	$\sqrt{2}$	0	0		
X_6^-	2	−2	0	$\sqrt{2}$	$-\sqrt{2}$	0	0	−2	2	0	$-\sqrt{2}$	$\sqrt{2}$	0	0		
X_7^-	2	−2	0	-$\sqrt{2}$	$\sqrt{2}$	0	0	−2	2	0	$\sqrt{2}$	$-\sqrt{2}$	0	0		

						$L(\frac{1}{2}\frac{1}{2}\frac{1}{2})$								
					$\overline{C}_{2e}$	$\overline{C}_{2b}$						$\overline{\sigma}_{de}$	$\overline{\sigma}_{db}$	
			C_{31}^+	$\overline{C}_{31}^-$	$\overline{C}_{2f}$	C_{2e}			S_{61}^-	$\overline{S}_{61}^+$		$\overline{\sigma}_{df}$	σ_{de}	
	E	$\overline{E}$	C_{31}^-	$\overline{C}_{31}^+$	$\overline{C}_{2b}$	C_{2f}	I	$\overline{I}$	S_{61}^+	$\overline{S}_{61}^-$		σ_{db}	σ_{df}	
L_5^+	1	−1	−1	1	i	−i	1	−1	−1	1		i	−i	
L_6^+	1	−1	−1	1	−i	i	1	−1	−1	1		−i	i	
L_4^+	2	−2	1	−1	0	0	2	−2	1	−1		0	0	
L_5^-	1	−1	−1	1	i	−i	−1	1	1	−1		−i	i	
L_6^-	1	−1	−1	1	−i	i	−1	1	1	−1		i	−i	
L_4^-	2	−2	1	−1	0	0	−2	2	−1	1		0	0	

			$W(\frac{1}{2}\frac{1}{4}\frac{3}{4})$				
						$\overline{C}_{2d}$	$\overline{\sigma}_z$
						C_{2f}	$\overline{\sigma}_y$
			C_{2x}	S_{4x}^-	$\overline{S}_{4x}^+$	$\overline{C}_{2f}$	σ_z
	E	$\overline{E}$	$\overline{C}_{2x}$	S_{4x}^+	$\overline{S}_{4x}^-$	C_{2d}	σ_y
W_6	2	−2	0	$\sqrt{2}$	$-\sqrt{2}$	0	0
W_7	2	−2	0	$-\sqrt{2}$	$\sqrt{2}$	0	0

References

1. Drozdov, A.P.; Kong, P.P.; Minkov, V.S.; Besedin, S.P.; Kuzovnikov, M.A.; Mozaffari, S.; Balicas, L.; Balakirev, F.F.; Graf, D.E.; Prakapenka, V.B.; et al. Superconductivity at 250 K in lanthanum hydride under high pressures. *Nature* **2019**, *569*, 528–531. [CrossRef]
2. Somayazulu, M.; Ahart, M.; Mishra, A.K.; Geballe, Z.M.; Baldini, M.; Meng, Y.; Struzhkin, V.V.; Hemley, R.J. Evidence for Superconductivity above 260 K in Lanthanum Superhydride at Megabar Pressures. *Phys. Rev. Lett.* **2019**, *122*, 027001. [CrossRef] [PubMed]
3. Peng, F.; Sun, Y.; Pickard, C.J.; Needs, R.J.; Wu, Q.; Ma, Y. Hydrogen Clathrate Structures in Rare Earth Hydrides at High Pressures: Possible Route to Room-Temperature Superconductivity. *Phys. Rev. Lett.* **2017**, *119*, 107001. [CrossRef] [PubMed]
4. Sun, D.; Minkov, V.S.; Mozaffari, S.; Sun, Y.; Ma, Y.; Chariton, S.; Prakapenka, V.B.; Eremets, M.I.; Balicas, L.; Balakirev, F.F. High-temperature superconductivity on the verge of a structural instability in lanthanum superhydride. *Nat. Commun.* **2021**, *12*, 6863. [CrossRef]
5. Zhang, X.; Zhao, Y.; Li, F.; Yang, G. Pressure-induced hydride superconductors above 200 K. *Matter Radiat. Extrem.* **2021**, *6*, 068201. [CrossRef]

6. Yi, S.; Wang, C.; Jeon, H.; Cho, J.H. Stability and bonding nature of clathrate H cages in a near-room-temperature superconductor LaH_{10}. *Phys. Rev. Mater.* **2021**, *5*, 024801. [CrossRef]
7. Kruglov, I.A.; Semenok, D.V.; Song, H.; Szczęśniak, R.; Wrona, I.A.; Akashi, R.; Davari Esfahani, M.M.; Duan, D.; Cui, T.; Kvashnin, A.G.; et al. Superconductivity of LaH_{10} and LaH_{16} polyhydrides. *Phys. Rev. B* **2020**, *101*, 024508. [CrossRef]
8. Krüger, E. Constraining Forces Stabilizing Superconductivity in Bismuth. *Symmetry* **2018**, *10*, 44. [CrossRef]
9. Blum, V.; Gehrke, R.; Hanke, F.; Havu, P.; Havu, V.; Ren, X.; Reuter, K.; Scheffler, M. Ab initio molecular simulations with numeric atom-centered orbitals. *Comput. Phys. Commun.* **2009**, *180*, 2175–2196. [CrossRef]
10. Havu, V.; Blum, V.; Havu, P.; Scheffler, M. Efficient O(N)O(N) integration for all-electron electronic structure calculation using numeric basis functions. *Comput. Phys. Commun.* **2009**, *228*, 8367–8379. [CrossRef]
11. Bradley, C.; Cracknell, A.P. *The Mathematical Theory of Symmetry in Solids*; Claredon: Oxford, UK, 1972.
12. Krüger, E.; Strunk, H.P. Group Theory of Wannier Functions Providing the Basis for a Deeper Understanding of Magnetism and Superconductivity. *Symmetry* **2015**, *7*, 561–598. [CrossRef]
13. Krüger, E. Superconductivity Originating from Quasi-Orbital Electrons III. Quasi-Orbital Conduction Electrons in Non-Adiabatic Systems. *Phys. Status Solidi B* **1978**, *90*, 719–731. [CrossRef]
14. Streitwolf, H.W. *Gruppentheorie in der Festkörperphysik*; Akademische Verlagsgesellschaft Geest & Portig KG: Leipzig, Germany, 1967.
15. Kostrzewa, M.; Szczęśniak, K.M.; Durajski, A.P.; Szczęśniak, R. From LaH_{10} to Room–Temperature Superconductors. *Sci. Rep.* **2020**, *10*, 1592. [CrossRef] [PubMed]
16. Bi, J.; Nakamoto, Y.; Zhang, P.; Shimizu, K.; Zou, B.; Liu, H.; Zhou, M.; Liu, G.; Wang, H.; Ma, Y. Giant enhancement of superconducting critical temperature in substitutional alloy (La,Ce)H9. *Nat. Commun.* **2022**, *13*, 5952. [CrossRef] [PubMed]
17. Kong, P.; Minkov, V.S.; Kuzovnikov, M.A.; Drozdov, A.P.; Besedin, S.P.; Mozaffari, S.; Balicas, L.; Balakirev, F.F.; Prakapenka, V.B.; Chariton, S.; et al. Superconductivity up to 243K in the yttrium-hydrogen system under high pressure. *Nat. Commun.* **2021**, *12*, 5075. [CrossRef] [PubMed]
18. Chen, W.; Semenok, D.V.; Huang, X.; Shu, H.; Li, X.; Duan, D.; Cui, T.; Oganov, A.R. High-Temperature Superconducting Phases in Cerium Superhydride with a T_c up to 115*K* below a Pressure of 1 Megabar. *Phys. Rev. Lett.* **2021**, *127*, 117001. [CrossRef]